THE FAST SATELLITE FIELDS INSTRUMENT

R. E. ERGUN*, C. W. CARLSON, F. S. MOZER, G. T. DELORY, M. TEMERIN, J. P. McFADDEN, D. PANKOW, R. ABIAD, P. HARVEY, R. WILKES and H. PRIMBSCH
Space Sciences Laboratory, University of California, Berkeley, CA, U.S.A.

R. ELPHIC
Los Alamos National Laboratory, Los Alamos, NM, U.S.A.

R. STRANGEWAY
University of California, Los Angeles, CA, U.S.A.

R. PFAFF
Goddard Space Flight Center, Greenbelt, MD, U.S.A.

C. A. CATTELL
University of Minnesota, Minneapolis, MN, U.S.A.

Abstract. We describe the electric field sensors and electric and magnetic field signal processing on the FAST (Fast Auroral SnapshoT) satellite. The FAST satellite was designed to make high time resolution observations of particles and electromagnetic fields in the auroral zone to study small-scale plasma interactions in the auroral acceleration region. The DC and AC electric fields are measured with three-axis dipole antennas with 56 m, 8 m, and 5 m baselines. A three-axis fluxgate magnetometer measures the DC magnetic field and a three-axis search coil measures the AC magnetic field. A central signal processing system receives all signals from the electric and magnetic field sensors. Spectral coverage is from DC to ~4 MHz. There are several types of processed data. *Survey data* are continuous over the auroral zone and have full-orbit coverage for fluxgate magnetometer data. *Burst data* include a few minutes of a selected region of the auroral zone at the highest time resolution. A subset of the burst data, *high speed burst memory data*, are waveform data at 2×10^6 sample s^{-1}. Electric field and magnetic field data are primarily waveforms and power spectral density as a function of frequency and time. There are also various types of focused data processing, including cross-spectral analysis, fine-frequency plasma wave tracking, high-frequency polarity measurement, and wave-particle correlations.

1. Introduction

The primary scientific goal of the FAST mission is to investigate auroral electron acceleration, ion heating, and wave-particle interactions (Temerin *et al.*, 1990). These phenomena involve a rich variety of plasma processes which include electrostatic shocks (Mozer *et al.*, 1977), double layers (Temerin *et al.*, 1982), field-

*Currently at the Department of Astrophysical and Planetary Sciences and the Laboratory for Atmospheric and Space Physics, University of Colorado, Boulder, CO, U.S.A.

Space Science Reviews **98:** 67–91, 2001.

aligned electrons (McFadden *et al.*, 1986), Langmuir and whistler wave emissions (Gurnett *et al.*, 1969), auroral kilometric radiation (AKR) (Gurnett, 1974), ion conics (Klumpar, 1986), ion beams, and the formation of the auroral density cavity. The FAST mission was designed to have one to three orders of magnitude higher time resolution than previous auroral satellite missions which have identified many of the auroral processes but were unable to resolve them fully.

The FAST satellite was launched into an $\sim 83^\circ$ inclination orbit with a 350 km perigee and 4175 km apogee in August, 1996. The satellite is oriented in a 'cart-wheel' attitude which has the spin axis nearly (negative) normal to the orbital plane. It is spin stabilized with a spin period of 5 s. The satellite crosses the auroral zones (which form ovals at $\sim 65^\circ - 70^\circ$ magnetic latitude North and South) four times an orbit. The orbit was designed to have a Northern apogee during January and February of 1997 for coordinated ground-based and optical observations.

In situ observations of auroral processes at high resolution require high data rates from all instruments which would exceed telemetry capability. Because the auroral zones are only a fraction of the FAST orbit, it is possible to acquire data at many times the maximum telemetry rate if the data are stored on-board. Central to the FAST satellite is a large ($\sim$128 MByte) solid state memory common to all instruments.

The FAST data system is described elsewhere (Harvey *et al.*, 2001) so we provide only a brief overview. The on-board memory accepts two primary types of science data from all instruments: *survey data* which have continuous coverage over the entire auroral zone and *burst data* which have only a few minutes of coverage (corresponding to $\sim$500 km of ground track) at the highest resolution. The position of the auroral zone, $\sim 65^\circ - 70^\circ$ magnetic latitude, varies enough that on-board triggers are required for the burst data. Survey data has three sub-types: 'full-orbit' data which is typically for the fluxgate (DC) magnetometer only, 'slow survey' which has $\sim$0.06 s resolution waveforms in the sub-auroral and polar cap regions, and 'fast survey' which typically has $\sim$0.5 ms resolution.

The basic plan of operation is as follows. The FAST satellite always acquires magnetic field data. As it approaches auroral latitudes, the science instruments are put into 'slow survey' by a time-tagged command. Once the auroral electron precipitation is detected, the science instruments are configured into 'fast survey'. If signals of scientific interest are seen by the burst triggers, burst data is collected for between $\sim$5 s to several minutes. Collection typically includes 25% of data prior to the trigger. There may be several burst collections depending on the available memory. The survey and burst data are stored on board until telemetered to ground.

The Fields Instrument includes the electric field and magnetic field sensors, the electric and magnetic field signal processing, and a wave-particle correlator. This article will detail the electric field sensors and the electric and magnetic field signal processing system. The magnetic field sensors (Elphic *et al.*, 2001), and the wave-particle correlator (Ergun *et al.*, 1998), and the booms (Pankow *et al.*, 2001) are described in separate articles.

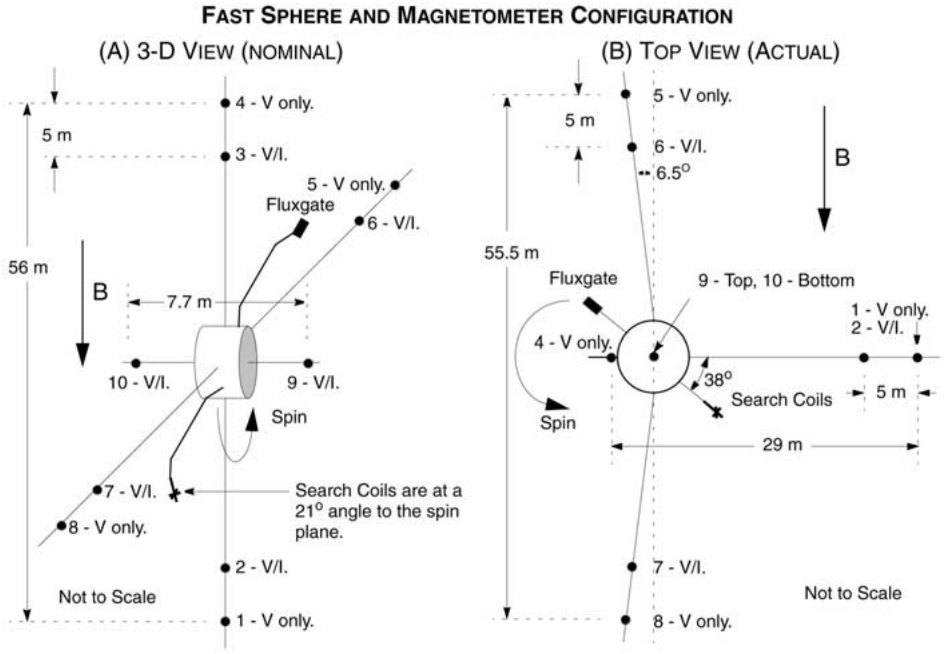

Figure 1. (a) A three-dimensional view of the electric and magnetic field sensors on the FAST satellite as designed. The electric field instrument has eight spherical sensors that are on four wire booms (two each) in the spin plane and two that are on rigid axial booms. All of the spherical sensors can operate in 'voltage mode' (marked with 'V') in which they measure the local plasma potential with respect to the payload. The electric field signals are measured by pairs of sensors which form 56 m, 7.7 m, or 5-m dipoles. Six of the ten sensors, marked with 'I', can operated in current mode where the electron current is measured for deriving plasma density. The fluxgate and search coil magnetometers are on ∼2-m booms. The search coil assembly is rotated 21° out of the spin plane. (b) The deployed state. The wire boom carrying sensors 3 and 4 did not fully deploy.

2. Fields Instrument Overview

The Fields Instrument has a number of sensors and signal processing subcomponents that are designed to produce the survey and burst data in accordance with the FAST data system. In this section, we briefly describe subcomponents of the Fields Instrument and show how they are linked together to provide full spectral coverage of electric and magnetic fields. The subcomponents are described in detail in Sections 3–5.

2.1. SENSORS

Figure 1 diagrams the electric and magnetic field sensors in their nominal (Figure 1(a)) and actual (Figure 1(b)) positions. There are ten spherical sensors for measuring the electric field. Eight sensors are on four wire booms (one of which did not fully deploy) in the spin plane and two are on rigid booms that are deployed

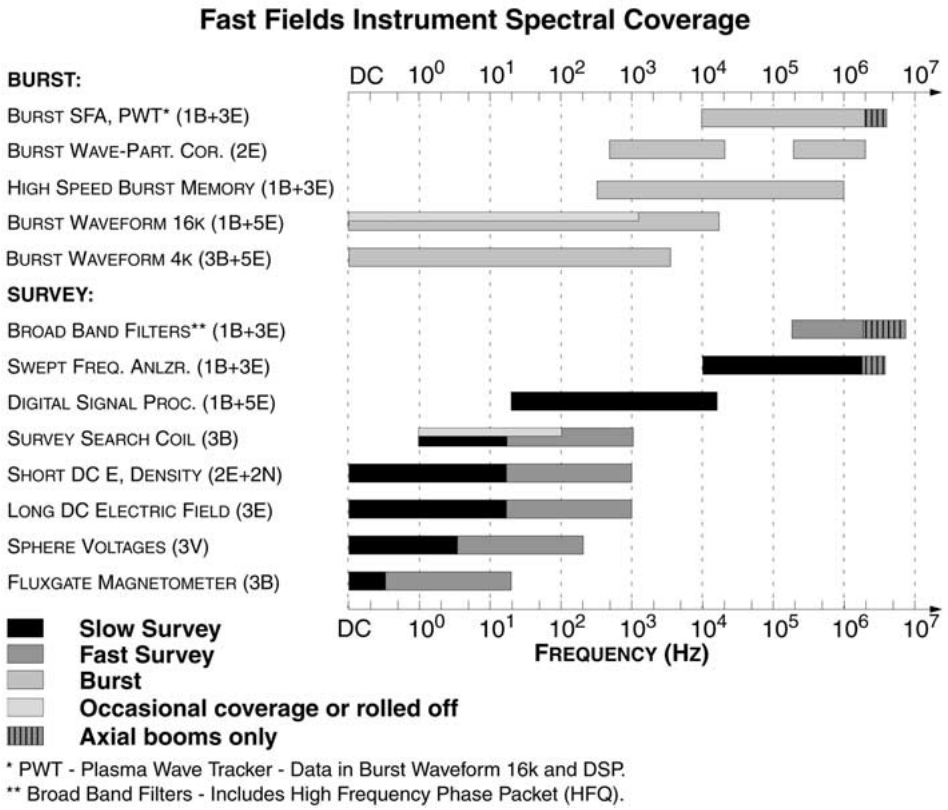

Figure 2. The spectral coverage of fields instrument.

along the spin axis. The vector DC and AC electric field signals are derived from the voltage difference between pairs of spherical probes which form dipoles of 5 m or 56 m in the spin plane (Mozer, 1973). The spin-plane wire booms have two sensors each to make multi-point measurements which can be used to determine the wave vector of coherent emissions with cross-spectral analysis. The tip-to-tip length of the spin axis dipole is 7.7 m. Six of the ten sensors can operate as Langmuir probes, measuring the electron current to a probe at a fixed potential to determine the electron density.

The DC magnetic field (to ∼100 Hz) is measured by a three-axis fluxgate magnetometer and the AC magnetic fields are measured by three search coils (∼10 Hz to 4 kHz on two axes, ∼10 Hz to 500 kHz on one axis). The fluxgate magnetometer is on a 2-m boom opposite an identical boom which carries the search coils. The satellite is oriented so that the magnetic field lies within 6° of the spin plane in the auroral regions.

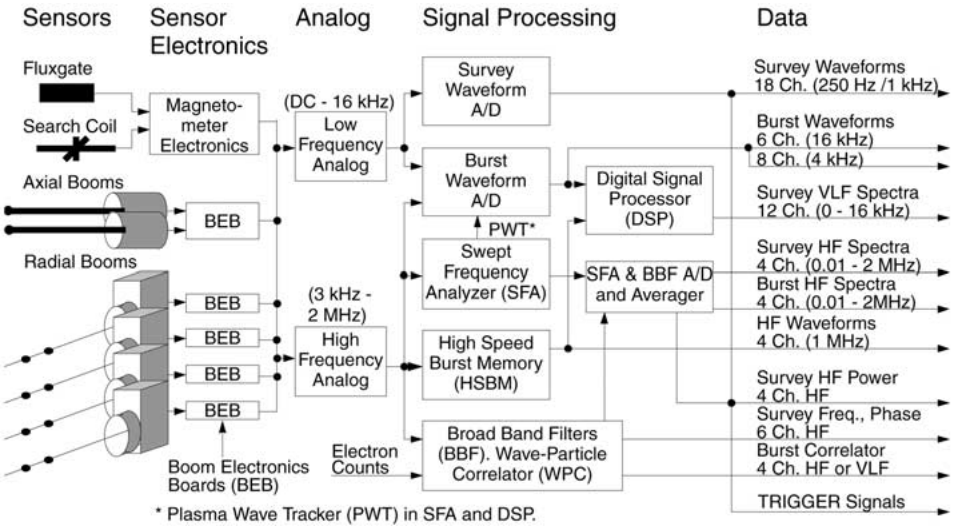

Figure 3. A block diagram of the fields instrument.

2.2. SPECTRAL COVERAGE

The Fields Instrument was designed to provide full spectral coverage (DC to 2 MHz) of electric and magnetic fields continuously as survey data (Figure 2). The lowest frequency data (up to 1 kHz) are vector waveforms of electric and magnetic fields, and waveforms of plasma density. The DSP (Digital Signal Processor) produces wave spectra from 16 Hz to 16 kHz and the SFA (Swept Frequency Analyzer) produces wave spectra from ∼10 kHz to 2 MHz. DSP and SFA spectra have ∼4 s resolution in slow survey and typically ∼0.25 s resolution in fast survey. The BBF (Broad Band Filters) provide high time resolution amplitude, frequency, and polarization of >200 kHz coherent wave signals in fast survey only.

Burst data (Figure 2) supplement the survey data with 16 kHz Nyquist-frequency waveforms, high time resolution SFA spectra (62.5 ms), PWT (Plasma Wave Tracker), and WPC (Wave-Particle Correlator) data. In addition, the HSBM (High-Speed Burst Memory) records four channels of waveforms, typically three E and one B, with a frequency range from ∼1 kHz to 1 MHz.

2.3. SIGNAL PROCESSING

Boom Electronics Board (BEB)

Figure 3 shows a functional overview of the Fields Instrument. The signals from the spherical sensors are passed through a BEB located at the boom deployment unit. The BEB supplies bias currents to the electric field sensors, controls the boom motors during deployment, and provides housekeeping signals to the instrument processor.

Low Frequency Analog and High Frequency Analog
The 16 electric and magnetic field sensors share a common signal processing system that is located in the central instrument electronics box. The signals are fed to two analog conditioning circuits. The low frequency analog conditioning covers the frequency band from DC to ∼16 kHz and the high frequency analog conditioning typically covers the frequency range from ∼3 kHz to 2 MHz (4 MHz maximum). The analog conditioning circuits have differential amplifiers to form the electric field signals from pairs of sensors and filters to isolate configured frequency bands. Analog switches and analog multiplexors allow the instrument to operate in a variety of modes.

Survey Waveforms
Survey waveforms (Figure 3) include 18 electric and magnetic field signals. The survey waveforms have maximum sample rates of 2048 samples s^{-1} (10 such channels at ∼1 kHz Nyquist) and 512 samples s^{-1} (8 such channels ∼250 Hz Nyquist).

Burst Waveforms
The burst waveforms unit has 8 A/D converters at 32 768 samples s^{-1} (∼16 kHz Nyquist). It operate in one of two modes. One mode has 8 signals at 32 768 samples s^{-1}. The other has 6 signals at 32 768 samples s^{-1} and 8 signals at 8196 samples s^{-1} (∼4 kHz Nyquist). Survey and burst waveforms are labeled by the band width: 16 kHz, 4 kHz, 1 kHz, or 250 Hz.

Digital Signal Processor (DSP)
Continuous coverage of the power spectral density of the 16 kHz signals is computed onboard by the DSP (Figure 3) which averages several Fast Fourier Transforms (FFT). The 1024 point FFT covers the frequency range from DC to ∼16 kHz with 32 Hz bandwidth and ∼100 dB dynamic range. The DSP can also perform a cross-spectral analysis to determine the phase difference of pairs of signals. The spectra produced by the DSP are treated as survey data, giving continuous coverage in the auroral zone.

Swept Frequency Analyzer (SFA)
High-frequency signals (>16 kHz) are processed three ways (Figure 3). The SFA produces power-frequency-time spectra typically from ∼10 kHz to 2 MHz (the sweep range is adjustable) with ∼80 dB dynamic range and 15 kHz bandwidth. The time resolution is typically 62.5 ms per spectra (31.25 ms is the fastest resolution) which are transmitted as burst data. Averaged spectra (125 ms to 4 s resolution) form survey data. The SFA unit also contains a Plasma Wave Tracker (PWT) which gives fine frequency (∼50 Hz) resolution over a narrow frequency range (16 kHz) that lies between 0 and 2 MHz.

High-Speed Burst Memory (HSBM)
The HSBM digitizes four high-frequency signals (∼3 kHz–1 MHz) at 2×10^6 samples s^{-1} with 10-bit resolution. HSBM data are stored in 2.5 Mbyte buffers that cover ∼0.25 s periods. Data intervals are selected by dedicated triggers which monitor wave power in both the high-frequency (200 kHz–2 MHz) and low-frequency (∼1 kHz–16 kHz) bands. The HSBM has very limited time coverage (<1% duty cycle) due to the high data rates.

Broad-Band Filters (BBF)
The BBF rectify four electric or magnetic field signals to determine the amplitude envelope of 200 kHz–2 MHz wave emissions versus time (∼1 ms resolution). They have a dynamic range of ∼60 dB. For the same four signals, the number of zero crossings are counted, which represents the wave frequency of narrow-band emissions. The phase shift between each pair of the four selected high-frequency signals (six phase difference signals) are also measured on board to determine the high-frequency wave polarization. The high-frequency wave amplitudes, zero crossing rates, and polarizations are telemetered as survey data.

Wave-Particle Correlator
The wave-particle correlator uses two electric or magnetic field signals and twelve of the stepped electron electrostatic analyzer anode signals (Carlson *et al.*, 1998a) to measure oscillations in electron fluxes in one of two selected frequency ranges. The low frequency range is from ∼500 Hz to ∼16 kHz and the high frequency range is from ∼200 kHz to ∼2 MHz. The correlation function is computed onboard by digital circuitry.

3. Electric Field Sensors, Booms, Preamplifiers, and Boom Electronics Board

3.1. Antennas and Sensors

The sensors for measuring the electric field are shown in Figure 1. The 8-cm diameter spherical probes contain electronics that operate in one of two selectable modes. All of the sensors can operate in 'voltage mode' in which they measure the potential of the nearby plasma with respect to the spacecraft. In voltage mode the probes are biased with a fixed current. Six of the sensors (marked with 'I' Figure 1) can operate in 'current mode' as Langmuir probes which measure plasma current. In current mode, the probe is biased at a fixed potential.

The radial booms are 2.5 mm diameter wires which support the sensors and carry power and signals between the sensors and the spacecraft. The wires have a kevlar braid that surrounds two coaxial cables and eight insulated wires. The kevlar braid is covered with aluminized kapton and a silver coated copper wire

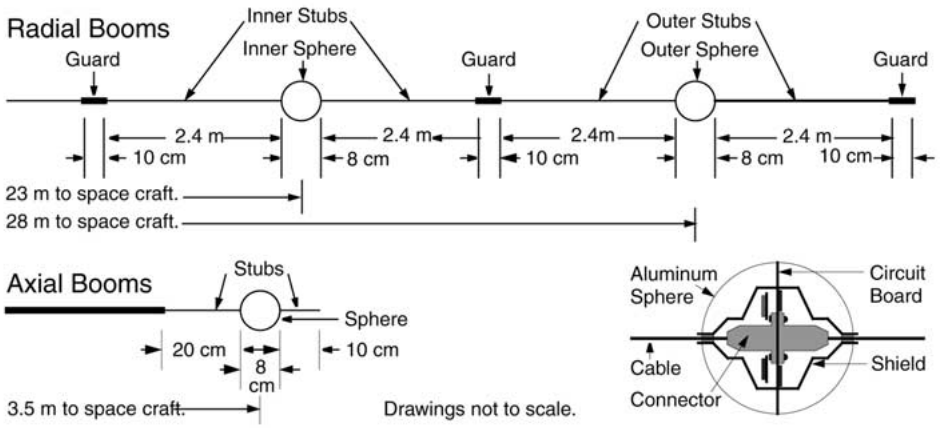

Figure 4. Top: the physical layout of the radial boom spheres, stubs, and guards. There are two spheres on each wire separated by 5 m. The 8-cm diameter spheres house a preamplifier. The outer sphere operates in voltage mode only. The inner sphere (nearer the spacecraft) operates in voltage or current mode. Adjacent to each sphere are 2.4-m stub sections which are biased at a selectable voltage with respect to the sphere potential. Three 10-cm long guard sections are also shown. Bottom left: the axial boom physical layout. There is one sphere on each ∼4-m rigid boom. Each sphere has a 20-cm stub on the inside and a 10-cm stub on the outside. The axial spheres can operate in voltage or current mode. Bottom right: the mechanical sphere assembly. Inside of each sphere are one or two circuit boards for voltage mode and/or current mode operation. Surrounding the circuitry and the wires is a shield which penetrates ∼0.2 cm beyond the sphere. The shield is driven at the sphere potential over the full bandwidth, thus reducing any unwanted capacitance between the sphere surface and the electronics to less that 1 pF. The shield also reduces cross talk between spheres to a negligible level.

braid which is exposed to the plasma. The exposed conductor is segmented into several sections that have controlled potentials. Figure 4 is a detailed diagram of the wire boom sensors.

The electric field is derived from the difference in potential between two probes in voltage mode. The probe potential is determined by a balance of electron current, ion current, photo-electron emission, secondary electron emission, and a bias current (Mozer, 1973). The probe surfaces are coated with carbon that produces known photo-emission characteristics. Bias currents are adjusted from −100 nA to 100 nA in steps of ∼0.8 nA to minimize errors. Bias tables for low and high plasma densities, eclipse and sun, and spacecraft configuration are stored on-board and are automatically adjusted as the spacecraft passes through the terminator.

The ‘stubs’ are 2.4 m sections of wire exposed to the plasma immediately beside the sphere. A stub section is added to the outside of the outer sphere for symmetry. The outer conductive surface of the stubs are driven at a fixed potential with respect to the sphere that is adjustable from −2.5 V to 2.5 V. By holding the stub potentials fixed with respect to the nearby sphere, the photo emission current between the sphere and the nearby wires can be controlled so that photo emission modulations

on the wire minimally effect the potential of the sphere. The voltage control of the stubs is resistively coupled to maintain electrical stability.

The three 'guards' are 10-cm sections immediately beside the stubs. The potentials of the guards are adjustable from -10 V to 0 V with respect to the outer most probe potential. The guards are typically biased at -5 V to restrict photoemission current between the spacecraft and the spherical probes and between the two probes. Optimized stub and guard biases are also stored in the on-board bias tables.

The spin axis booms are rigid, 4-m stacers that have a single sphere with short (20-cm and 10-cm) stubs and no guards. The preamplifier design of the axial spheres is identical to the inner radial spheres. The axial probes can operate in voltage or current mode.

3.2. PREAMPLIFIERS

Plasma resistance to the spherical probes is expected to vary from $\sim 10^6$ Ω to $> 10^9$ Ω and the capacitive coupling to the plasma is typically ~5 pF. Preamplifiers located inside the spherical probes are designed to have very low stray capacitance ($<$1.0 pF) and very high input resistance ($> 10^{11}$ Ω) so that electric fields from DC to ~2 MHz can be measured. An aluminum shield (Figure 4) electrically shields the probe surface from the circuitry inside the probe and the wire which runs through the probe. The same cover also provides radiation shielding. Radial and axial preamplifier response is diagramed in Figure 5(a) and the signal processing coverage of the electric field is diagramed in Figure 5(b). Signals less than ~300 Hz are typically resistively coupled to the plasma while those greater than ~300 Hz are typically capacitively coupled to the plasma. The drop in preamplifier gain to 0.8 at frequencies greater than 300 Hz is due to the cross over from resistive to capacitive coupling.

In current mode, sensors 6, 7, 9, and 10 have a dynamic range from ~0.5 nA to 2×10^4 nA representing a density range from ~0.2 cm^{-3} to ~104 cm^{-3} with typical auroral electron temperatures (~1 eV). Spheres 2 and 3 measure from ~10 nA to 5×10^5 nA for low-altitude coverage. The bias voltages on sensors 2, 3, 6, and 7 can be set between 0 V and 20 V with respect to one of two base potentials: (1) the nearby voltage mode sensor or (2) the potential derived from 0.8 the nearby voltage sensor and 0.2 the spacecraft potential. Initial testing on orbit has shown the first base potential can cause undesirable spacecraft charging so the latter base potential is always used. Sensors 9 and 10 are always referenced from the payload and can be biased from -5 V to 45 V.

3.3. BOOM ELECTRONICS BOARDS (BEBS)

A BEB is located in each of the four wire boom deployment units and one is located on the radiation shield of the main spacecraft to control the axial booms. The boom electronics boards perform the following functions: (1) receive commands from the

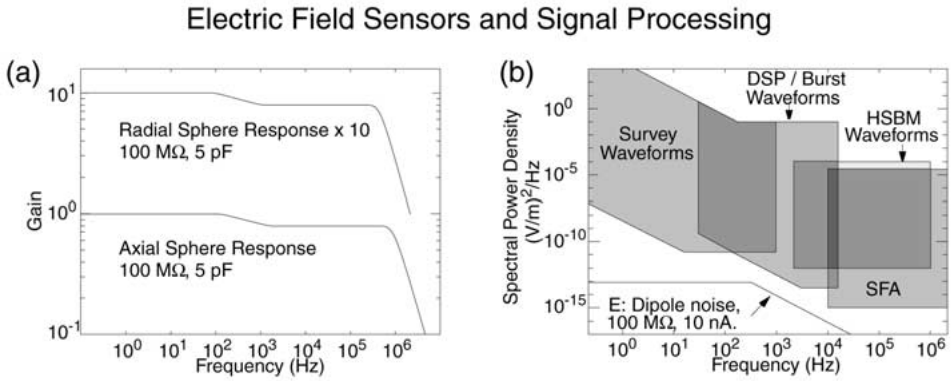

Figure 5. (a) The sensor preamplifier response as a function of frequency under 100 MΩ, 5 pF source impedance. The drop of gain from 1.0 to 0.8 at ∼300 Hz represents the cross over from resistive to capacitive coupling. The response on radial booms has an effective a two-pole roll off at ∼500 kHz due to losses driving the 28-m cable. The axial boom (2-m cable) preamplifier response has twice the bandwidth. (b) The theoretical noise level of the 56-m electric field antenna system and the dynamic range of survey waveform, DSP, SFA, and HSBM signal processing systems.

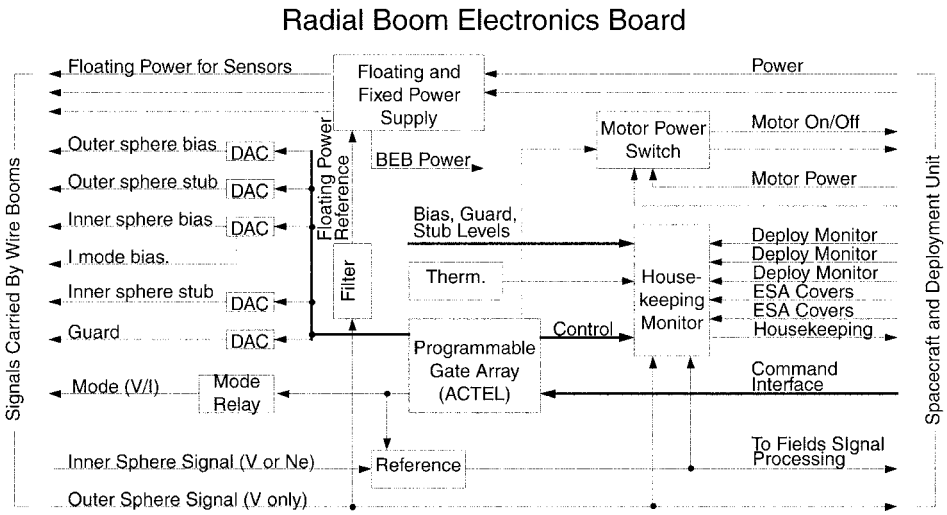

Figure 6. A block diagram of the radial boom electronics board.

instrument data processing unit (IDPU) including bias levels for the sensors, stubs, and guards, (2) provide analog bias voltages and currents to the sensors, (3) provide power to the sensor preamplifiers, (4) distribute the analog signals from the sensors to the fields signal processing system, (5) turn on and off wire boom motors from IDPU command, and (6) return housekeeping signals of bias levels, temperatures, and the state of deployment of the wire booms.

A block diagram of the radial BEB is in Figure 6. Commands from the IDPU are sent by a serial interface to a programmable gate array (all programmable gate

arrays in FAST are Actel 1020 series) which contains all of the digital logic. Each BEB has a unique address so that it can be individually commanded. Commands include the bias, guard, and stub levels which are fed to an 8-bit digital to analog converter (DAC).

A floating power converter provides power for the BEB and the sensor preamplifers. The sensor power supply has a reference to the sensor potential with a range from -52 V to 52 V. The DC to $\sim$300 Hz dynamic range of the sensors is from ~ -45 V to 45 V which can measure ± 1.6 V m^{-1} on the 56-m dipoles and $+11$ V m^{-1} on the 8-m axial dipole. The 5-m dipoles saturate at the same electric field amplitudes as the 56-m dipoles, except for short wavelength emissions. The sensors have a operating range of ~ -8 V to 8 V for signals $>\sim$ 300 Hz. The 56-m and 5-m dipoles can measure up to 300 mV/m wave electric fields and the 7.7-m axial dipole can measure up to 2 V m^{-1} wave electric fields.

4. Signal Processing and Data Products

We start with a discussion of science modes (Section 4.1). The signal processing descriptions are organized following the diagram in Figure 3: (4.2) survey waveforms, (4.3) burst waveforms, (4.4) DSP: LF spectra, (4.5) SFA: HF spectra, (4.6) PWT, (4.7) HSBM: HF digital waveforms, (4.8) BBF: HF power, frequency, and phase, and (4.9) the wave-particle correlator. Several signal processing systems may share common resources. For example, the digital signal processor uses burst waveform data to produce the survey spectra.

4.1. Science modes

The FAST instruments were defined under the concept of science 'modes', whereby the instruments can be configured to emphasize specific scientific investigations. Science modes also allow for optimizing investigations at various local times and altitudes as well as performing follow up investigations of any phenomena discovered during the mission. For example, a science mode that studies auroral kilometric radiation would emphasize the high-frequency signal processing. Another use of the modes is to control the overall data rate.

The Fields Instrument was designed with several layers of flexibility to accommodate a variety of science modes. The first layer of flexibility is in the sensor configuration. Six of the ten electric field sensors can be operated in one of two configurations. Next, a series of multiplexors allows selection of raw sensor signals, differential (electric field) signals, search coil magnetometer signals, and the fluxgate magnetometer signals into several signal processing systems. Finally, each of the signal processing systems has a variable data rate. The configuration of the sensors, the signal selection, and the individual data rates of each signal processing system are the main elements of a science mode.

4.2. SURVEY WAVEFORMS

All of the survey waveform signals share a single 16-bit A/D converter (Crystal Semiconductor CS5016) that constantly samples at 32 768 samples s^{-1}. The signals are filtered with 4-pole Bessel filters (1 kHz or 250 Hz) that are in a hybrid package ($\sim$1 g, 7.2 mW each). The survey waveform conversion rate is configurable by factors of two from 16 samples s^{-1} to 2048 samples s^{-1} for the 1 kHz waveforms, and from 4 samples s^{-1} to 512 samples s^{-1} for 250 Hz waveforms. The signals are under-sampled except at the maximum rate.

Eighteen low-frequency analog signals are processed as survey waveforms:

- Three long-baseline DC electric field signals (1 kHz).
- Four configurable signals that are either short baseline DC electric field signals, sensor voltages, or Langmuir probe (plasma density) outputs (1 kHz).
- Three sensor voltages (250 Hz).
- Three DC fluxgate magnetometer signals (250 Hz).
- Three AC search coil signals (1 kHz).
- Two LF ($\sim$1 kHz–16 kHz) wave power signals (128 Hz).

The signal selection, sensitivities, dipole lengths, and the dynamic range of the survey signals are summarized in Table I. The signals that are most often selected in the science modes are shaded. Electric field measurement and Langmuir probe data are plotted in panels (a) and (b) of Figure 12.

The three-axis fluxgate magnetometer signals are converted at rates from 16 samples s^{-1} to 2048 samples s^{-1} before being input into a recursive digital filter that is in a programmable gate array. The recursive filter acts as a one-pole low-pass filter at $f_0 = -\ln(15/16) f_{\text{sample}}/2\pi$, which is $\sim$21 Hz at maximum sample rate. The output rate of the fluxgate magnetometer signals are at $\frac{1}{4}$ the sample rate varying from 4 samples s^{-1} at the minimum rate to 512 samples s^{-1} at the maximum rate. Fluxgate magnetometer data are plotted in Figure 12(c).

4.3. BURST WAVEFORMS

There are eight 16-bit (Crystal Semiconductor CS5016) A/D converters dedicated to burst waveforms which simultaneously sample at 32 768 samples s^{-1}. Up to 14 signals out of 40 signals (Table II) can be selected for A/D conversion. Signal selection is set in the science mode. Two of the eight A/D converters can be configured to operate in two different ways. Each can sample one signal at 32 768 samples s^{-1} ($\sim$16 kHz Nyquist) or four signals at 8196 samples s^{-1} ($\sim$4 kHz Nyquist). The burst waveforms can come in one of two configurations: (1) eight waveforms at 32 768 samples s^{-1} or (2) six waveforms at 32 768 samples s^{-1} and eight at 8196 samples s^{-1}. Wave-forms sampled at 32 768 samples s^{-1} are filtered by 6-pole, 16 kHz Butterworth filters in hybrid packages. Waveforms sampled at 8196 samples s^{-1} are filtered by a 4-pole, 4 kHz Bessel filter in hybrid packages.

Table II summarizes the available signals and their properties. The entries ending with HG are AC coupled, high-gain signals with a frequency band from $\sim$3 kHz

TABLE I

Survey electric and magnetic field waveforms

Svy. packet	1 kHZ waveform E	Dipole (m)	Sensitivity (mV m^{-1})	Range (V m^{-1})	Alt.: Plasma Density	Range (nA)	Alt.: Sensor Volt	Range (v)	Alt.: Waveform	Dipole (m)	Range (V m^{-1})
1 1	**V1–V4**	29									
2 1	**V5–V8**	56	0.05	± 1.6							
3 1	**V9–V10**	7.7	0.36	± 11	Ne9	0.5–2×10^4	V9	± 45			
4 2	**V1–V2**	5	0.5	± 1.6	Ne2	10–5×10^5	V2	± 45	V1-V3	28	± 1.6
5 2	**V3–V4**				Ne3		V3	± 45	V2-V4	23	± 1.6
6 2	V5–V6	5	0.5	± 1.6	**Ne6**	0.5–2×10^4	V6	± 45	V5-V7	51	± 1.6
7 2	V7–V8	5	0.5	± 1.6	**Ne7**	0.5–2×10^4	V7	± 45	V6-V8	51	± 1.6

Svy. Packet	1 kHz Waveform Search	Search Coil Length	Sensitivity (nT-Hz)	Range (nT-Hz)
8 3	**Mag1ac**	7″	8.1×10^{-2}	$\pm 2.7 \times 10^3$
9 3	**Mag2ac**	7″	8.1×10^{-2}	$\pm 2.7 \times 10^3$
10 3	**Mag3ac**	21″	4.2×10^{-2}	$\pm 1.4 \times 10^3$

Svy. Packet	205 Hz Signals	Freq. Range (kHz)	Range Minimum (mV m^{-1})	Range Maximum (mV m^{-1})	205 Hz Plasma Density	Range (nA)	250 Hz Sensor Volt	Range (v)
11 3							**V4**	± 45
12 3							**V8**	± 45
13 3					Ne10	0.5–2×10^4	**V10**	± 45
14 3	**VLF1**	1-16	0.01	200				
15 3	**VLF2**	1-16	0.01	200				

Svy. Packet	DC Waveform Fluxgate	Sensitivity (nT)	Range (G)
16 1	**Mag1dc**	2	± 0.6
17 1	**Mag2dc**	2	± 0.6
18 1	**Mag3dc**	2	± 0.6

to 16 kHz. The high-pass filter at 3 kHz has one pole. Otherwise, the signals are DC coupled. The sensitivity in Table II is the one-bit level, while the range is limited either by the maximum range of the sensor or the A/D converter. A/D converters 7 and 8 can be multiplexed to receive four 4 kHz bandwidth signals. If the signal is available at 4 kHz, an ‘m’, standing for ‘multiplexed’, is added (e.g., 8 m). Otherwise the signal is available at 16 kHz. A typical configuration is

TABLE II

	Signal E	Dipole (m)	Sensitivity (μV m^{-1})	Range* (V m^{-1})	A/D		Signal	Sensitivity (mV nA^{-1})	Range (V nA^{-1})	A/D band
1	**V1-V4HG**	29	4.7	± 0.2	1	21	V1	1.37	± 45	1
2	**V1-V2HG**	5	27.5	± 1.1	5	22	V2	1.37	± 45	5
3	V3-V4HG	–	–	–	6	23	V3	1.37	± 45	6
4	**V5-V8HG**	56	2,5	± 0.1	2	24	V4	1.37	± 45	3
5	V1-V4	29	95	±v1.6	1,8 m	25	V5	1.37	± 45	2
6	V5-V8*	56	49	± 1.6	2,8 m	26	V6	1.37	± 45	7
7	**V9-V10**	7.7	357	± 11	3,8	27	V7	1.37	± 45	8
8	V1-V2*	5	549	± 1.6	5,7 m,8 m	28	V8	1.37	± 45	4
9	V3-V4*	–	–	–	6,7 m.8 m	29	V9	1.37	± 45	4
10	V5-V6*	5	549	± 1.6	7,7 m,8 m	30	V10	1.37	± 45	8 m
11	V7-V8*	5	549	± 1.6	8,7 m,8 m	31	Ne2	10	5×10^5	5
12	V1-V3*	28	98	± 1.6	5,7 m,8 m	32	Ne3	–	–	6
139	V2-V4*	23	120	± 1.6	6,7 m.8 m	33	Ne6	0.5	2×10^4	7,7 m,8 m
14	V5-V7*	51	54	± 1.6	7,7 m,8 m	34	Ne7	0.5	2×10^4	8,7 m,8 m
15	V6-V8*	51	54	± 1.6	8,7 m,8 m	35	Ne9	0.5	2×10^4	4
16	VQUAD	–	–	–	7,8 m	36	Ne10	0.5	2×10^4	8 m

	Signal B	Search Coil	Sensitivity (nT-Hz)	Range (nT-Hz)	A/D		Signal	(See BBF)	A/D Band
17	**Mag1ac**	7″	8.7×10^{-2}	2850	7 m	37	BBF1		
18	**Mag2ac**	7″	8.7×10^{-2}	2850	7 m	38	BBF2		
19	**Mag3ac**	21″	4.2×10^{-2}	1376	4,6,7 m	39	BBF3		
20	**PWT**		See SFA	–	–	40	BBF4		

shaded. VQUAD is the measurement of the quadrupole signal (V1+V4−V5−V8). PWT, the plasma wave tracker, and the BBF channels described later.

The burst digital data are continuously available to the instrument data processing unit and to the DSP at an overall data rate of 4.194 Mbit s^{-1}. The periods of data capture are selected by the instrument data processor. The selection criteria are from trigger signals supplied by the Fields Instrument and the particle detectors.

4.4. DIGITAL SIGNAL PROCESSOR: LF SPECTRA

The primary function of the DSP is to provide continuous coverage of the spectral power density of the electric and magnetic field in the frequency range up to 16 kHz. It also has three other optional functions: provide spectral power density of the high-frequency (∼1 kHz to 1 MHz) electric and magnetic field, perform cross-spectral analysis of the low-frequency and high-frequency electric field pairs,

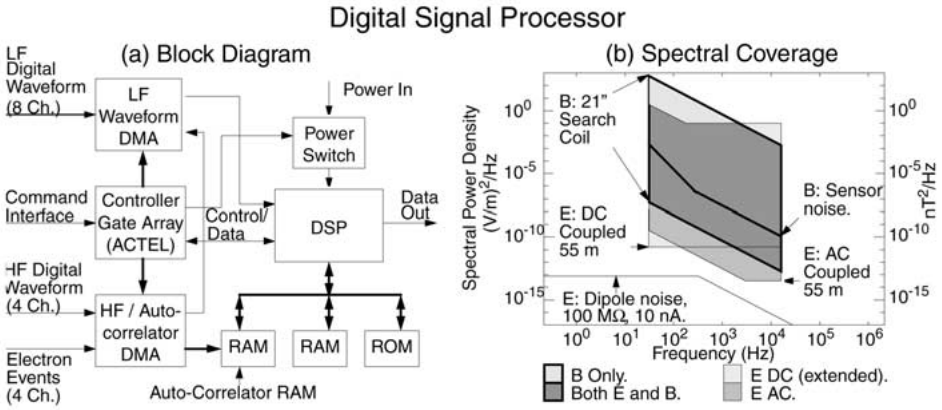

Figure 7. (a) A block diagram of the DSP. The DSP receives data from the burst A/D converters (low-frequency), the HSBM (high-frequency), and the electron electrostatic analyzers. The primary function of the DSP is to provide continuous 16 Hz–16 kHz wave power spectra in the auroral zone. (b) The dynamic range coverage versus frequency for DSP spectra. The DSP averages FFTs of electric and magnetic waveforms. The time resolution of the 1024 point FFTs varies from 31 ms to 4 s.

and calculate the auto-correlation function of four fixed energy channels from the electron spectrographs.

The LF spectrum analysis averages 2^n (n is configurable from 0 to 7), 1024-point Fast Fourier Transforms (FFT) of the digital waveforms from the burst A/D converters. The resulting spectra have 32 Hz resolution in frequency and from 32 ms to 4 s resolution in time. The selection, sensitivity, and range of the burst waveforms are described in Table II.

A block diagram of the DSP is in Figure 7(a). The eight burst waveforms are fed into a dedicated Direct Memory Access (DMA) designed into a programmable gate array. A second custom DMA was designed to access the high speed burst memory waveforms (1 MHz waveforms at 2 Msamples s^{-1}) and four channels of the electron spectrograph. All of the data passes from the DMAs into the RAM through single high-speed serial interface in the DSP. In all, there are sixteen inputs which are individually selectable.

A third programmable gate array acts as a controller. Its primary functions are to (1) direct start up, reprogramming, and resets of the DSP, (2) receive commands from the instrument data processing unit (IDPU), (3) provide timing and control of the DMAs, (4) detect single event latch up, single event upset, or malfunction of the DSP and restart, and (5) hardware protect the code area in RAM.

The DSP processor is a 32-bit floating point ATT-DSP32C with an input clock at 32 MHz (below the 50 MHz maximum). Radiation testing, performed at the University of California at Berkeley, determined that the total dose tolerance exceeds 200 kRad. Four radiation hardened static CMOS RAMs were used to make a 32-bit by 32 Kbit memory. Bi-polar ROMs are used to hold the code.

Due to the high power consumption (2.5 W) and slow access speed (100 ns) of the ROMs, the start-up sequence copies the ROM code into the RAM code area then turns off the ROMS. The code can be augmented or patched by the IDPU. The code area is hardware protected after the start-up sequence is completed.

The dynamic range of the DSP LF spectra are displayed in Figure 7(b). The data are logarithmically compressed to 8 bits. The electric field spectra range from 2×10^{-13} (V m^{-1})^2 Hz^{-1} to 2×10^{-3} (V m^{-1})^2 Hz^{-1} on the 56-m high gain (V5-V8HG) signal. The 5m DC-coupled signals have a dynamic range starting at 10^{-10} (V m^{-1})^2 Hz^{-1}. The range of the signal processing is optimized for auroral processes which are well above the sensor noise levels. The magnetic spectra of the $21''$ search coil range from $\sim 1 \times 10^{-10}$ (nT)^2 Hz^{-1} to $\sim 5 \times 10^{-3}$ (nT)^2 Hz^{-1} at 1 kHz. The search coil dynamic range is limited by the sensor noise at frequencies greater than ~500 Hz. Auroral electric field spectra from the DSP are displayed in Figure 12(f).

4.5. Swept frequency analyzers: HF spectra

All high-frequency signals are from the high-frequency analog unit (Figure 3) which is co-located with the SFA. The high-frequency analog unit has AC-coupled differential amplifiers which form electric field signals and analog switches for mode configuration. Table III describes selection and the sensitivities of the signals.

The primary functions of the SFA are (1) to provide continuous coverage of the high-frequency (~10 kHz–2 MHz) electric and magnetic fields as survey data, (2) provide high time resolution (62.5 ms) spectra of the electric and magnetic fields as burst data, and (3) provide fine frequency resolution observations of narrow-band emissions such as auroral kilometric radiation. The third function is designated as the Plasma Wave Tracker.

A block diagram of one SFA channel is given in Figure 8(a). The SFA has four channels. In three of the channels, the high-frequency signal is passed into a 3-pole low-pass filter at 2 MHz. The fourth channel, which can be used by the plasma wave tracker, has a 4 MHz filter. The filtered signal is mixed with a sweeping reference (10.7–12.7 MHz in normal operation), passed through a 10.7 MHz crystal filter with 15 kHz bandwidth, then mixed again at 10.65 MHz to produce a 50 kHz intermediate frequency. The resulting signal is rectified and logarithmically amplified before digital (8-bit) conversion by the high-frequency A/D converter (see Figure 2). The 256-point HF spectra have ~8 kHz steps (over-sampling the 15 kHz band width) covering from 0 to 2 MHz. Since the sweeping reference is produce by a digital frequency synthesizer, the sweep can be configured to have maximum range of 500 Hz, 1 MHz, 2 MHz, or 4 MHz. The sweep rate can be configured to 31.25 ms or ~62.5 ms (typical operation).

The survey data are an average 2^n sweeps, where n is set from 0 to 7. The sweep rate changes from 'slow survey' to 'fast survey', usually from $n = 6$ to $n = 3$, thus increasing the data rate and time resolution of the sweeps (most often

TABLE III
HF signal processing

Ch.	Signal SFA	Dipole (m)	Sensitivity $(V\ m^{-1})^2\ Hz^{-1}$ $(nT^2\ Hz^{-1})$	Range $(V\ m^{-1})^2\ Hz^{-1}$ $(nT^2\ Hz^{-1})$	Frequency max. (MHz)	Alternative signal	Dipole (m)	Sensitivity $(V\ m^{-1})^2\ Hz^{-1}$	Range $(V\ m^{-1})^2\ Hz^{-1}$	Frequency max. (MHz)
1	V1-V4	29	4.0×10^{-15}	6.0×10^{-7}	2	V1-V2	5	2.0×10^{-13}	2.0×10^{-5}	2
2	V5-V8	56	1.0×10^{-15}	1.6×10^{-7}	2	V7-V8	5	2.0×10^{-13}	2.0×10^{-5}	2
3	Mag3ac	21″ SC	1.0×10^{-11}	1.0×10^{-4}	0.6	V5-V6	5	2.0×10^{-13}	2.0×10^{-5}	2
4	V9-V10	7.7	3.0×10^{-13}	3.0×10^{-5}	4	V3-V4	–	–	–	–
4						V1-V4	29	4.0×10^{-15}	6.0×10^{-7}	2
4						V1-V2	5	2.0×10^{-13}	2.0×10^{-5}	2

Ch.	Signal HSBM	Dipole (m)	Sensitivity $(V\ m^{-1})$ or (nT)	Range* $(V\ m^{-1})$ or (nT)	Frequency max. (MHz)	Alternative signal	Dipole (m)	Sensitivity $(V\ m^{-1})$	Range* $(V\ m^{-1})$	Frequency max. (MHz)
1	V1-V4	29	0.4	220	2	V1-V2	5	2.0	500	2
2	V5-V8	56	0.2	110	2	V7-V8	5	2.0	500	2
3	Mag3ac	21″ SC	4.0×10^{-3}	2.0	0.6	V5-V6	5	2.0	500	2
4	V9-V10	7.7	1.25	750	4	V3-V4	–	–	–	–

Ch.	Signal HF Power	Dipole (m)	Sensitivity $(V\ m^{-1})$ or (nT)	Range* $(V\ m^{-1})$ or (nT)	Frequency max. (MHz)	Alternative signal	Dipole (m)	Sensitivity $(V\ m^{-1})$	Range* $(V\ m^{-1})$	Frequency max. (MHz)
1	V1-V4	29	0.2	220	2	V1-V2	5	1.0	500	2
2	V5-V8	56	0.1	110	2	V7-V8	5	1.0	500	2
3	Mag3ac	21″ SC	2.0×10^{-3}	2.0	0.6	V5-V6	5	1.0	500	2
4	V9-V10	7.7	0.75	2000	4	V3-V4	–	–	–	–

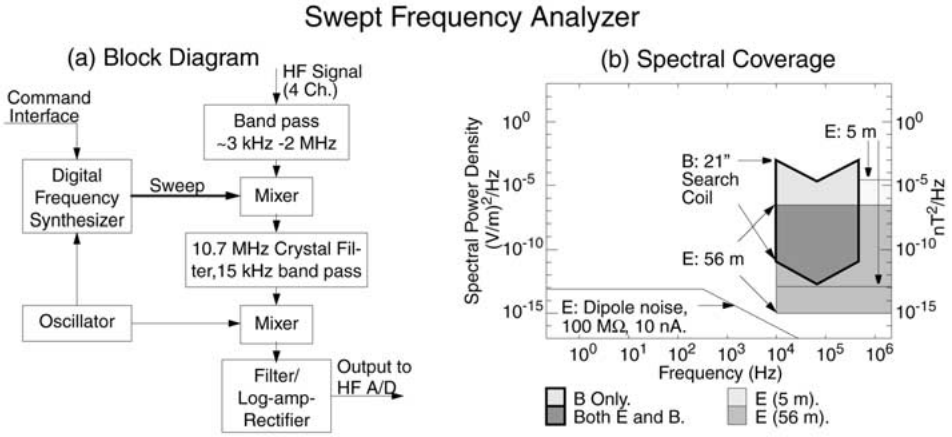

Figure 8. (a) A block diagram of the SFA. Three of the four channels are filtered to 2 MHz and one channel to 4 MHz. The latter channel can be used by the plasma wave tracker by setting the digital frequency synthesizer to a fixed frequency. (b) The spectral coverage and dynamic range of the SFA. The electric field range is from 10^{-15} (V m^{-1})^2 Hz^{-1} (56-m dipole) to 10^{-5} (V m^{-1})^2 Hz^{-1} (5-m dipole). The 21″ search coil has a peak sensitivity at ∼65 kHz with a frequency range to ∼600 kHz.

4 s in slow survey and 0.5 s in fast survey). Burst data transmits every sweep. The spectral coverage of the SFA is displayed in Figure 8(b). The usual gain setting in the auroral zone has a dynamic range from 10^{-15} to 10^{-7} (V m^{-1})^2 Hz^{-1} for electric fields and from 10^{-12} to 10^{-4} nT^2 Hz^{-1} (at 100 kHz) for magnetic fields. SFA data are displayed in Figure 12(e).

4.6. PLASMA WAVE TRACKER

The primary function of the PWT is to provide fine-frequency resolution spectra of narrow- band emissions. This is accomplished using the fourth channel of the SFA. The signal from the digital frequency synthesizer is set at a fixed frequency (f_0) that is (1) fixed by configuration, (2) dynamically set at the electron cyclotron frequency, or (3) dynamically set by the number of zero crossings in the wave form. The fixed frequency is the center of the 15 kHz band.

After passing through the 10 700 MHz crystal filter (Figure 8(a)), the signal passes to the second mixer which is set at 10 692 MHz when configured for the plasma wave tracker. The resulting signal (∼0.5 kHz to 15.5 kHz) represents the frequency band $f_0 - 7.5$ kHz to $f_0 + 7.5$ kHz. The PWT signal then is digitized as a burst waveform (see Table II, entry 20) and/or processed by the DSP. The frequency resolution of the PWT signal is limited by the jitter in the digital frequency synthesizer to +50 Hz. An example of PWT data is given in Figure 12(d).

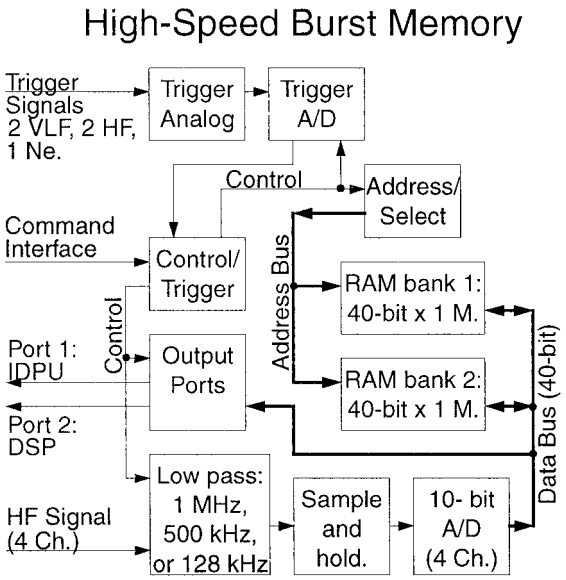

Figure 9. A block diagram of the HSBM. Four high-frequency channels are low-pass filtered then digitized. The data are selected by high- or low-frequency wave event or plasma density cavity by a dedicated trigger system and are stored in a 10 Mbyte RAM. The RAM buffers can be output as waveform data (Port 1) or transferred to the DSP which produces a average of FFTs.

4.7. HIGH SPEED BURST MEMORY: HF DIGITAL WAVEFORMS

The HSBM produces 0.5 μs resolution digital waveforms of four signals, typically three electric field and one magnetic field, with ~0.1% coverage in the auroral zone (~2 s out of 30 min). Alternatively, the HSBM can supply the DSP (described above) with digital HF waveforms to be converted into HF spectra. The HSBM is located in the Fields Instrument signal processing and is not part of the main instrument burst memory. A block diagram is in Figure 9. Signal selection and dynamic range are in Table III.

The HSBM has three main sub-systems. The analog section has selectable three-pole low-pass filters of 125 kHz, 500 kHz, and 1 MHz corresponding to three selectable A/D speeds of 250 ksample s^{-1}, 1 Msample s^{-1}, or 2 Msample s^{-1}. Four 10-bit MP7694 A/D converters are augmented with a high-speed sample and hold. The four A/D converters are on a 40-bit bus that is continuously written to a 10 Mbyte RAM. The trigger system uses the rectified and logarithmically amplified low-frequency wave power (see survey waveforms), the high-frequency wave power (see later), and the plasma density (see survey waveforms) as inputs. The trigger A/D converter alternately samples two of the selected inputs labeled 'trigger A' and 'trigger B', often set to one low-frequency and one high-frequency power level.

The digital logic is contained in three programmable gate arrays and works as follows. The RAM is divided into four buffers, one of which continuously accepts data (input buffer), two are holding buffers with the highest trigger A and trigger B levels, and the forth buffer outputs data (output buffer). If the trigger level exceeds the level in one of the holding buffers, the instrument (1) waits for $\frac{3}{4}$ of the input buffer to be written keeping $\frac{1}{4}$ of the buffer for data prior to the trigger event and (2) swaps the input buffer and a holding buffer thus overwriting the holding buffer. This process continues until the output buffer has been completely read. At that point, one of the holding buffers, alternating between the two, becomes the output buffer. The new holding buffer is assigned a zero trigger level.

The logical process above has several additional features. One can assign a minimum trigger level to the HSBM so that a trigger event cannot occur unless the minimum requirement is met. There are two settings of trigger position within the buffer keeping either $\frac{1}{4}$ or $\frac{1}{2}$ of the buffer for data prior to the trigger. The triggers can be set 'retriggerable' or 'absolute'. The former allows for a trigger event to restart if the trigger level increases later in the event so that the peak is always at the trigger position. The latter does not allow for a restart. The maximum buffer size is 2.5 Mbytes. The buffer sizes can be $1/2^n$ of the maximum with n between 0 and 7. Finally, on can go into 'time-based' triggering whereby the triggers events occur evenly in time rather than by plasma wave amplitude. The last feature is used when the DSP generating spectra.

4.8. Broad-band filters: HF power, frequency, and phase

The main function of the Broad-Band Filter (BBF) signal processing is to provide high-time resolution power, frequency, and phase information for high-frequency signals (Figure 10). Four AC-coupled, high-frequency signals are processed. The selection, sensitivities, and ranges are described in Table III. The selected signals are high-pass filtered at 200 kHz with a three-pole passive LCR filter. Since the sensor preamplifier response rolls off at ~500 kHz, the BBF emphasizes auroral kilometric radiation which falls in the 200 kHz to 500 kHz band. The four signals are rectified and pseudo-logarithmically amplified and then passed to the high-frequency A/D converter (Figure 3) at typically 1 ms resolution. The BBF has a 60 dB dynamic range.

The selected analog signals are also fed to a comparator producing a digital representation of the zero crossing. The digital signals are input to counters which yield the frequency of a dominating, narrow band signal. Six pairs of the digital signals are processed by a phase discriminator which measures the relative phase of the signals to determine wave polarization. The zero-crossing counters and the phase measurements have 4 ms time resolution.

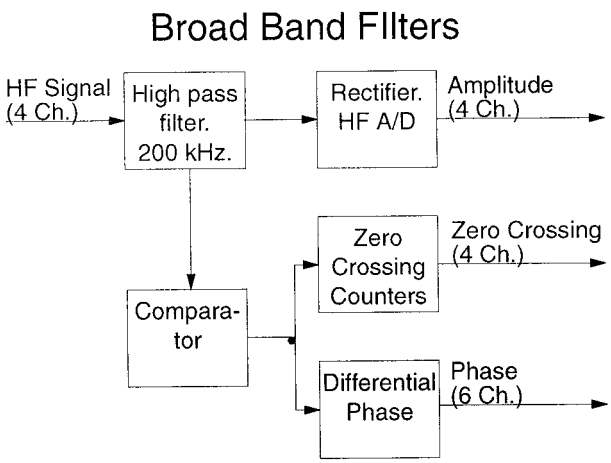

Figure 10. A block diagram of the broad band filter, phase, and zero crossing processing. Four high-frequency channels are high-pass filtered then rectified to measure the high-frequency wave amplitude at high time resolution. The high-frequency signals are digitized by a comparator.

4.9. WAVE-PARTICLE CORRELATOR

The main scientific objective of the wave-particle correlator instrument is to identify the energy and pitch angle of particles that are interacting with waves. Measurement of the amplitude of particle oscillations and their phase relation with the wave allows for the evolution of the wave and distribution function to be studied in detail. Wave-particle correlator instruments provide a direct observation of wave-particle interactions. The wave-particle correlator has been described in a previous article (Ergun *et al.*, 1998), so we do not provide a full description here.

The wave-particle correlator detects oscillations in particle flux by integrating the product of the wave electric field and particle flux (Ergun *et al.*, 1991a; Lin *et al.*, 1995). This technique can be used to determine both the amplitude and phase (with respect to the wave phase) of oscillatory currents. 'Resistive' currents are in phase with the electric field and determine energy flow between the wave and particles (Ergun *et al.*, 1991b), whereas 'reactive' currents are in phase with wave potential and can indicate nonlinear kinetic processes such as particle trapping (Muschietti *et al.*, 1994).

One channel of the wave-particle correlator is diagramed in Figure 11. The electric field signal from the antenna is filtered to the desired frequency band. The instrument has selectable pass bands of 200 kHz to 2 MHz for Langmuir wave and auroral kilometric radiation studies, and 500 Hz to 20 kHz for lower frequency wave studies. The filtered electric field signal is fed into an analog phase splitter which consists of two all-pass filters that have phase responses which differ by 90° over a broad frequency range. (An all-pass filter is a unity gain circuit that has a non-zero phase response.) The digital output of the comparator represents the

TABLE IV
FAST fields instrument: mass and power

Component	Sub Component	Number	Mass	Power	Duty cycle	Orbit averaged power
	Radial boom/sensors	4	3.1 kg			
	Radial BEB	4	0.5 kg	0.5 W		
Electric Field	Axial boom/sensors	2	1.6 kg			
BEB/sensors	Axial BEB	1	0.5 kg	0.5 W		
	Totals (regulated power)			2.5 W		
	Total (unregulated power)		18.1 kg	2.8 W	0.25	0.70 W
	Senor		0.87 kg	0.45 W		
Search coil	Boom		1.87 kg			
	Totals (unregulated power)		2.65 kg	0.60 W	0.25	0.15 W
	Sensor		0.63 kg			
Fluxgate	Boom		1.78 kg			
(not including	Dirver electronics		0.90 kg	1.51 W		
ACS sensor.)	Totals (unregulated power)		3.31 kg	2.01 W	1.00	2.01 W
Signal	LF analog and A/D converters		1.76 kg	2.22 W		
processing	HF analog and SFA		0.88 kg	1.92 W	1.00 x	
	Digital signal proc.		0.40 kg	1.28 W	0.35 W	
	High speed burst memory		0.55 kg	0.65 W	and	
	Wave-particle correlator		0.80 kg	1.75 W	0.25 x	
	Totals (regulated power)			7.82 W	10.1 W	
	Totals (unregulated power)		4.39 kg	10.43 W		2.88 W
Totals			28.45 kg	15.9 W		5.74 W

polarity of the wave signal. The comparator output is then digitally integrated with electron events to make the correlation function.

5. Fields Instrument Performance

The Fields Instrument has met or exceeded all of the design specifications as outlined above, with the exception of the boom deployment. The radial wires holding sensors 3 and 4 jammed during initial deployment; the cause of the jam is unknown. Sensor 4 is exposed to the plasma near the spacecraft while sensor 3 is undeployed and is fixed at spacecraft ground. The impacts were minimal because of the flexible design of the Field Signal processing. They are:

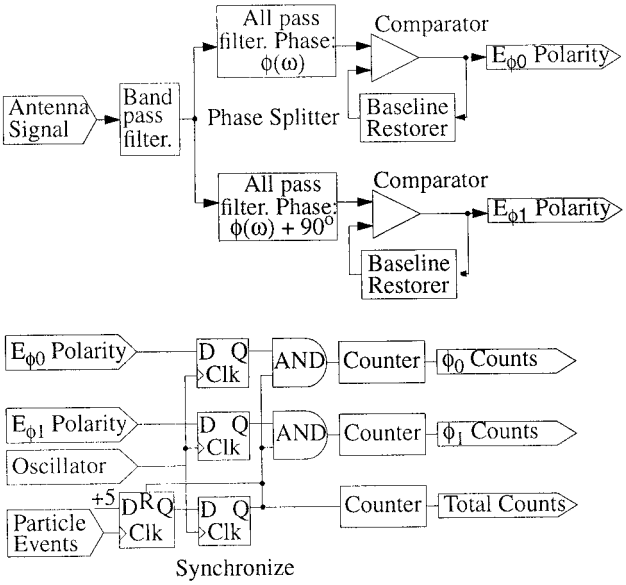

Figure 11. A simplified block diagram of a one channel wave-particle correlator. The electric field signal processing is diagrammed on top. Comparators produce two digital signals that represent polarities of the wave signal that has been split into two phases that differ by 90°. The wave polarity signals are correlated with the particle pulses (bottom) with digital logic. The ϕ_0*Count* (or ϕ_1*Count*) and is incremented only if the polarity of the ϕ_0 (or ϕ_1) wave signal is positive. The correlation measurements are ($2\phi_0$*Count - Total Count*) and ($2\phi_1$*Count - Total Count*).

- The DC (<300 Hz) contamination on sensor 4 was too high for scientific use. The spin-plane electric fields are calculated from linear combinations of signals V1, V5, and V8 (from Table I, signals 1, 2, and 5). There was little loss of accuracy and excellent scientific return (see Carlson *et al.*, 1998b, and references therein).
- The AC contamination on sensor 4 was remarkably low. Comparisons between V5-V8 and V1-V4 AC-coupled waveforms (burst and HSBM) and spectra (DSP and SFA) showed little or no increase in noise.
- Cross-correlation measurements are made between V5-V6 and V7-V8 which are not co-aligned. There was a loss of sensitivity in cross-spectral analysis.
- The sensor 10 axial boom deployment was delayed to avoid an a spin-axis tip of ∼2.2° during the early phase of the FAST mission.

6. Mass and Power

Table IV summarizes the mass and power for the Fields Instrument. The radial boom sensors include the deployment mechanism, two sensors, the wire booms, and support structure for the radiation shield. The axial boom and sensor mass does

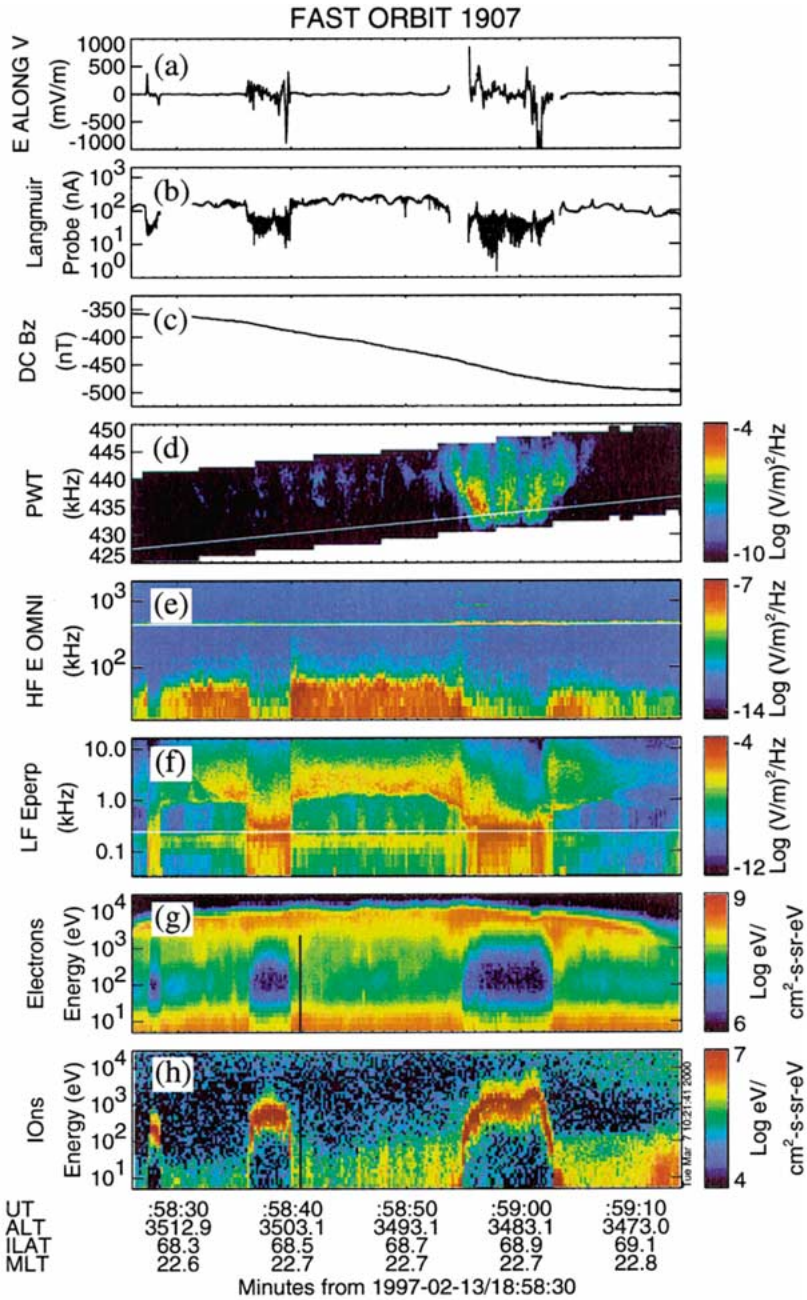

Figure 12. Data from the FAST satellite. (a) The DC electric field perpendicular to B projected along the velocity vector of the spacecraft. (b) The current to the Langmuir probe reflecting plasma density. Plasma density scales at $\sim$1 cm^{-3} to 1 nA. (c) The magnetic field along the pay-load spin axis (nearly West). (d) Fine-frequency resolution data from the Plasma Wave Tracker. The electron cyclotron frequency is also plotted. (e) Electric field power spectra from the Swept Frequency Analyzer. (f) Low-frequency emissions (DSP data). The H^+ cyclotron frequency is also plotted. (g) Electron and (h) ion data from the energetic particle detectors.

not include the transmitter support tubes. The majority of the signal processing and electric field sensors are nominally on for ∼25% of the orbit resulting in low orbit-averaged power consumption.

References

Carlson, C. W. *et al.*: 1998a, in R. R. Pfaff, J. E. Borovsky, and D. T. Young (eds.), 'Design and Applications of Imaging Plasma Instruments', *Measurement Techniques in Space Plasma*, AGU, Geophysical Monograph 102, p. 125.

Carlson, C. W., Pfaff, R. F., and Watzin, J. G.: 1998b, 'The Fast Auroral Snapshot Mission', *Geophys. Res. Lett.* **25**, 2013.

Ergun, R. E., Carlson, C. W., McFadden, J. P., Clemmons, J. H., and Boehm, L. H.: 1991a, 'Langmuir Wave Growth and Electron Bunching: Results From a Wave-Particle Correlator', *J. Geophys. Res.* **96**, 225.

Ergun, R. E., Carlson, C. W., McFadden, J. P., TonThat, D. M., Clemmons, J. H., and Boehm, M. H.: 1991b, 'Observation of Electron Bunching During Landau Growth and Damping', *J. Geophys. Res.* **96**, 11371.

Ergun, R. E., McFadden, J. P., and Carlson, C. W.: 1998, in R. F. Pfaff, J. E. Borovsky, and D. T. Young (eds.), 'Wave-Particle correlator Instrument Design', *Measurement Techniques in Space Plasmas* AGU Geophysical Monograph 102, p. 325.

Gurnett, D. A.: 1974, 'The Earth as a Radio Source: Terrestrial Kilometric Radiation', *J. Geophys. Res.* **79**, 4227.

Gurnett, D. A., Pfeiffer, G. W., Anderson, R. R. Mosier, S. R., and Cauffman, D. P.: 1969, 'Initial Observations of VLF Electric and Magnetic Fields with the Injun 5 Satellite', *J. Geophys. Res.* **74**, 4631.

Klumpar, D. M.: 1986, in T. Chang (ed.), 'A Digest and Comprehensive Bibliography on Transverse Auroral Ion Acceleration', *Ion Acceleration in the Magnetosphere and Ionosphere*, American Geophysical Union Monograph, p. 389.

Lin, R. P., Anderson, K. A., Ashford, S., Carlson, C., Curtis, D., Ergun, R., Larson, D., McFadden, J., McCarthy, M., Parks, G. K., Reme, H., Bosqued, J. M., Coutelier, J., Cotin, F., D'uston, C., Wenzel, K.-P., Sanderson, T. R., Henrion, J., Ronnet, J. C., and Paschmann, G.: 1995, 'A Three-Dimensional Plasma and Energetic Particle Investigation for the Wind Spacecraft', *Space Sci. Rev.* **71**, 125.

McFadden, J. P., Carlson, C. W., and Boehm, M. H.: 1986, 'Field-Aligned Electron Precipitation at the Edge of an Arc', *J. Geophys. Res.* **91**, 1723.

Mozer, F. S.: 1973, 'Analysis of Techniques for Measuring DC and AC Electric Fields in the Magnetosphere', *Space Sci. Rev.* **14**, 272.

Mozer, F. S., Carlson, C. W., Hudson, M. K., Torbert, R. B., Parady, B., Yatteau, J., and Kelley, M. C.: 1977, 'Observations of Paired Electrostatic Shocks in the Polar Magnetosphere', *Phys. Rev. Lett.* **38**, 292.

Temerin, M. A., Carlson, C. W., Cattell, C. A., Ergun, R. E., McFadden, J. P., Mozer, F. S., Klumpar, D. M., Peterson, W. K., Shelley, E. G., and Elphic, R. C.: 1990, in T. Chang *et al.*, (eds.), 'Wave-Particle Interactions on the FAST Satellite', *Physics of Space Plasmas (1989)*, p. 343, Scientific Publishers, Inc., Cambridge, MA.

Temerin, M., Cerny, K., Lotko, W., and Mozer, F. S.: 1982, 'Observations of Double Layers and Solitary Waves in the Auroral Plasma', *Phys. Rev. Lett.* **48**, 1175.